WIDEBAND RF CHANNELIZATION USING FREQUENCY-DEPENDENT BEAM STEERING OF FOCUSED BULK ACOUSTIC WAVES

F. Sabet-Peyman, K. Chau, and I.C. Chang

Litton Applied Technology
Sunnyvale, California 94088-3478

ABSTRACT

Development of wideband transducers coupled with frequency dependent beam steering of Bulk Acoustic Waves (BAW) in low loss single crystals provide a great opportunity for efficient channelization of broad band microwave signals. Due to material anisotropy, phase and group velocity collinearity represents in many instances a constraint that must be taken into account in a given design. The work presented in this paper deals with the diffraction process in BAW channelizers/spectrum analyzers in a general way. Our diffraction model is based on Huygen's principle to predict the pressure field in a longitudinal device for various input frequencies. The formulation is applied to compute generalized wave disturbances due to an apodized/unapodized linear phased input array and a curved reflector. The material is YAG where parabolic approximation to the slowness curve is valid for the required steering angles.

Channelization of RF signals based on dispersion and focusing of Bulk Acoustic Waves (BAW) in solid media, was proposed in 1984.[1] Subsequently, the preliminary experimental results were reported in 1984 and 1985.[2,3] Although the experimental devices were not optimized, their performance based on limited number of channels within the operation frequency range of 100 to 200 MHz was indeed encouraging. The proof-of-concept devices such as that shown in figure 1 were all made of fused silica, in order to minimize cost and simplify design and manufacturing process. In these devices, the acoustic waves are launched via a phased array of transducers, excited by the input RF signals. After traveling through the bulk acoustic media the dispersed beams are brought into focus at different spatial locations on the output transducer plane, where their amplitude and phase is detected. Under ideal conditions such as isotropy, the angular spectrum of the acoustic field on the focal plane of an aberration free reflector is similar to the far field pattern of a phased array antenna in free space.

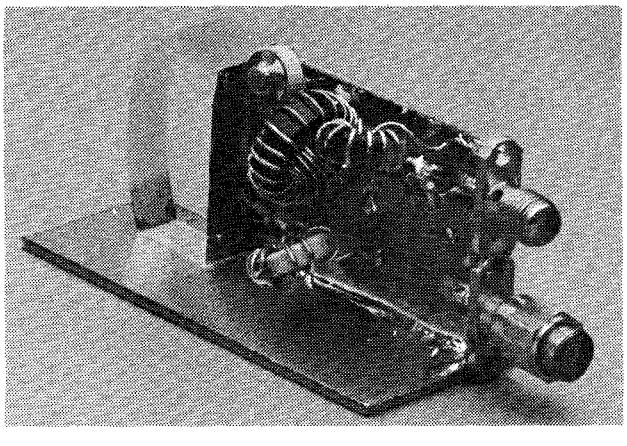

Figure 1. An experimental shear bulk acoustic wave channelizer made of fused silica.

For modern day EW applications wide instantaneous microwave bandwidth, high sensitivity and large dynamic range are required. While large fractional bandwidths are achievable by using platelet transducer technology,[4] one has to be concerned about reducing the level of crosstalk between adjacent channels and suppression of diffraction-induced spurious signals to achieve higher spurious free dynamic range. To minimize insertion loss at microwave frequencies, efficient crystals with proper orientation associated with the excited acoustic mode must be used. These materials, however, are generally anisotropic, where anisotropy depends on crystalline symmetry, mode and direction of ultrasonic wave propagation, and associated elasticity coefficients. The work presented in this paper deals with modeling the diffraction process in BAW channelizers/spectrum analyzers. Because of the relatively large angular dispersion of BAW, anisotropy and its variation with off-axis propagation angles must, therefore, be included in the design.

The concept of acoustic wave diffraction in anisotropic media has received much attention in the literature.[5,6,7,8] Most of the work dealing with bulk wave propagation utilizes Huygen's principle in order to calculate the resulting radiation fields. Our diffraction model is based on Huygen's formulation due to its mathematical and conceptual simplicity, coupled with its complete generality and numerical precision. The analysis proceeds in two steps. First, we find the amplitude and phase profiles at the reflector due to the input transducer array, and then compute the field at the output transducer plane. Referring to figure 2, The pressure at a point (x,y) inside the medium is written as[5]

0149-645X/86/0000-0569$01.00 © 1986 IEEE

$$p(x,y,t) = \text{Re}\left[\frac{i\omega\rho_o}{2\pi}\int_\sigma \frac{V(\xi,\eta)\,\exp i(\omega t - \bar{k}\cdot\bar{r})}{|r|}\,d\xi d\eta\right] \quad (1)$$

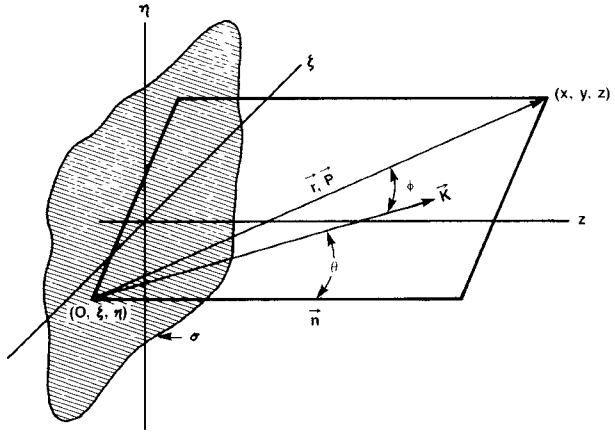

Figure 2. Geometry of ultrasonic diffraction in anisotropic media.

The integral is performed over the input transmitting aperture σ. $\bar{k}$ is the ultrasonic wave vector, ρ_o is the material density with ω and $V(\xi,\eta)$ defined as ultrasonic angular frequency and the initial particle velocity input amplitude along the propagation direction. The Poynting vector lies along $r = [(x - \xi), (y - \eta), z]$ which joins the input element of area $d\xi d\eta$ to the field point (x,y). The distance between the source and observation points is

$$|r| = [(x - \xi)^2 + (y - \eta)^2 + z^2]^{1/2} \quad (2)$$

Considering the input transducers to be independent piston-like sources, $V(\xi,\eta)$ can be expressed in terms of its normal component to transducer plane.

$$V(\xi,\eta) = V_N(\xi,\eta)\cos\theta = V_N(\xi,\eta)\left(\frac{z}{r}\right) \quad (3)$$

where θ is measured from the transducer normal, $\bar{n}$.

For anisotropic materials the direction of energy flax vector $\bar{p}$ (Poynting vector) deviates from that of the wave front normal $\bar{k}$. The propagation vector $\bar{k}$ lies in the plane of $\bar{p}$ and the transducer normal $\bar{n}$, making an angle θ with $\bar{n}$ and angle ϕ with $\bar{p}$.

Waterman[9] has shown that the ultrasonic propagation velocity v of longitudinal waves along a direction close to a pure-mode axis in the cubic, hexagonal, tetragonal, and trigonal crystals deviates from v_o along the axis by a term proportional to θ^2,

$$v = v_o(1 - \gamma\theta^2) \quad (4)$$

where γ is a constant dependent upon the elastic moduli and the direction of $\bar{n}$, and v_o is the pure mode acoustic velocity. For propagating directions close to a three, four, or six fold pure-mode axis in elastically anisotropic media, the longitudinal ultrasonic wave vector magnitude $k(\theta)$ is

$$k(\theta) = k_o(1 + \gamma\theta^2) \quad (5)$$

derived by Papadakis.[5] The basic assumption is that the anisotropy parameter, γ, is constant over the range of the propagation angle, θ, and $\gamma\theta \ll 1$. Energy will propagate at an angle ϕ with respect to $\bar{k}$ and obeys the relation

$$\tan\phi = \frac{-1}{k}\frac{\partial k}{\partial\theta} \quad (6)$$

Assuming that ϕ is small and neglecting the higher order terms in θ, equation (6) reduces to

$$\phi \approx -2\gamma\theta \quad (7)$$

using (5) and (7), for small θ, the dot product $\bar{k}\cdot\bar{r}$ becomes[6]

$$\bar{k}\cdot\bar{r} = k_o r(1 + \gamma\theta^2)\cos\phi \approx k_o r[1 + \gamma(1 - 2\gamma)\theta^2] \quad (8)$$

substituting (8) into (1) and taking the real part will lead to

$$p(x,y,z;t) = \frac{\omega\rho_o}{2\pi}\int_\sigma V_N(\xi,\eta)\,\frac{z}{r^2}\sin\{\omega t - k_o r[1 + \gamma(1 - 2\gamma)\theta^2]\}\,d\xi d\eta \quad (9)$$

Trigonometric identities reduce this to

$$p(x,y,z;t) = \frac{z\omega\rho_o}{2\pi}\sin\omega t \int_\sigma \frac{V_N(\xi,\eta)\cos k_o r\,[1 + \gamma(1 - 2\gamma)\theta^2]\,d\xi d\eta}{r^2} - \frac{z\omega\rho_o}{2\pi}\cos\omega t \int_\sigma \frac{V_N(\xi,\eta)\sin k_o r\,[1 + \gamma(1 - 2\gamma)\theta^2]\,d\xi d\eta}{r^2} \quad (10)$$

Equation (10) can simply be expressed as

$$P = A\sin\omega t - B\cos\omega t = C\cos(\omega t + \delta) \quad (11)$$

where at a distance z from the aperture plane,

$$A(x,y,z) = \frac{z\omega\rho_o}{2\pi} \int_\sigma V_N(\xi,n) \cos k_o r[1 + \gamma (1 - 2\gamma)\theta^2] \, d\xi dn \quad (12a)$$

$$B(x,y,z) = \frac{z\omega\rho_o}{2\pi} \int_\sigma V_N(\xi,n) \sin k_o r [1 + \gamma (1 - 2\gamma)\theta^2] \, d\xi dn \quad (12b)$$

$$C(x,y,z) = [A^2(x,y) + B^2(x,y)]^{1/2} \quad (12c)$$

$$\delta(x,y,z) = \tan^{-1} \left[\frac{A}{B}\right] \quad (12d)$$

It has already been demonstrated that phase variations over the transducer surface contribute to an apparent attenuation.[10] Consequently it is important to determine the phase variations for different channels as a function of output transducer's location and size.

The field distribution at the reflector, $P_i(x,y)$, can be computed by straight forward application of (11) and (12) for any form of initial velocity distribution. Since the reflector is large compared to the beam height, it introduces no additional diffraction effects. However, reflection efficiency of the reflector will vary depending on the angle of incidence. Upon reflection, part of the incident wave front will be converted to shear waves. The conversion efficiency (loss) at each point will depend on the spatial coordinates and other factors such as shear/longitudinal mode phase velocities and angle of incidence. Amplitude reflectivity for incident longitudinal beams is given by

$$r_L(x,y) = \frac{Vs^2(x,y) \sin 2\beta_L \sin 2\beta_s - V_L^2(x,y) \cos^2 2\beta_s}{V_s^2(x,y) \sin 2\beta_L \sin 2\beta_s + V_L^2(x,y) \cos^2 2\beta_s} \quad (13)$$

The subscripts L and s refer to longitudinal and shear waves respectively, β_L and β_s are reflected beam angles with respect to the reflector normal at coordinal (x,y), where the incident and reflected angles for longitudinal beams are assumed equal in magnitude. If the free boundary is unaberrated, the reflected amplitude would be:

$$P_r(x,y) = r_L(x,y) \, P_i(x,y) \quad (14)$$

the same computation process is repeated for the reflected wave fronts in order to determine the pressure field at the output plane.

We use the formulation developed to compute the pressure field intensities at the output transducer plane. The bulk acoustic material is YAG for its low attenuation. The input is a loo element linear phased transducer array of radiators similar to that shown in figure 3. Figure 4

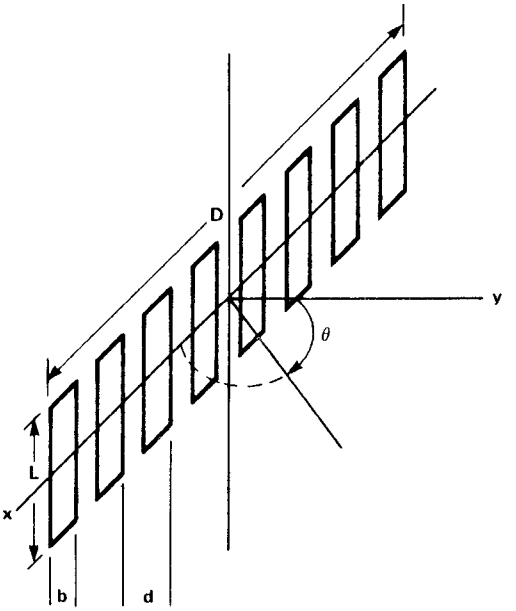

Figure 3. Design of linear input array of aperture size D x L center separation d = 20 microns, element size b = 10 microns, and the total number of elements is 100.

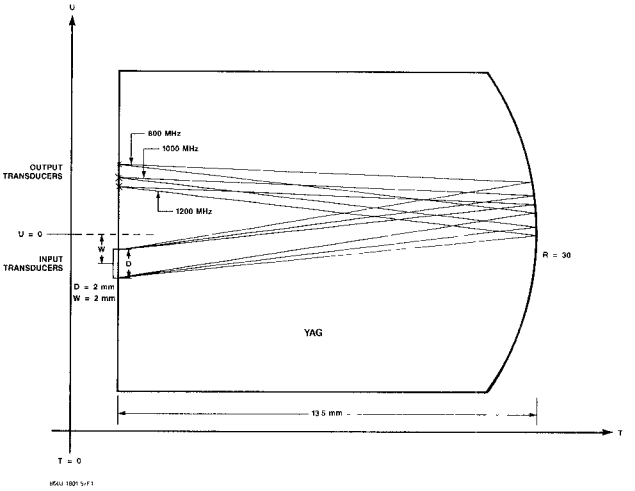

Figure 4. Illustration of the particular configuration used in the computations.

illustrates in some detail the exact geometry of the experimental system where all future discussions are referenced to it.

The field intensities are directly computed by using (11) and (12) for 3 input frequencies of 800, 1000, and 1200 MHz. Figure 5 is the decibel

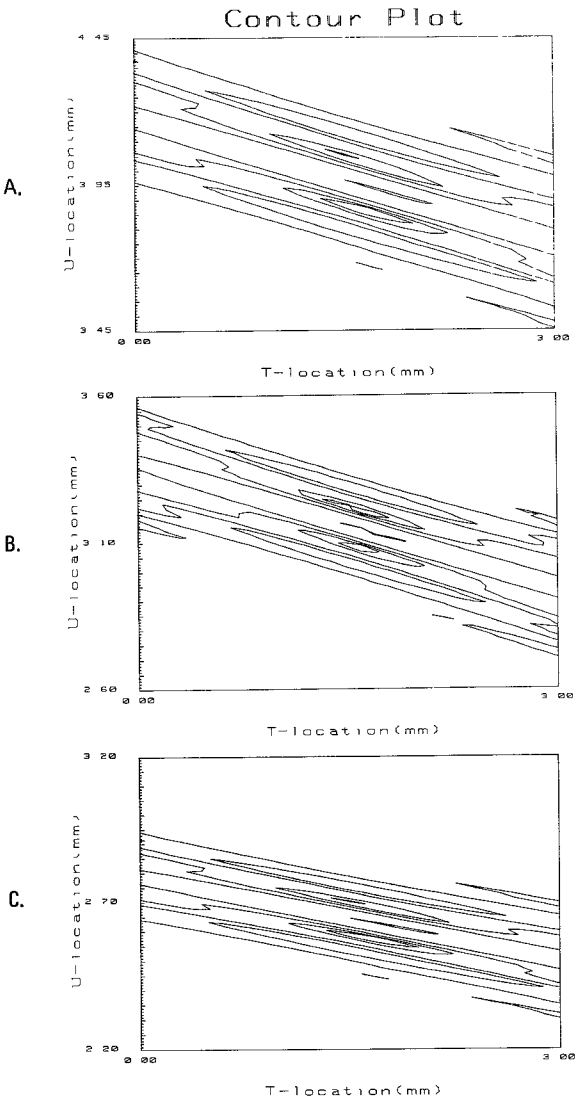

Figure 5. Decibel contour plot of field intensity in the vicinity of output transducer plane of figure 4.
A - At the input frequency of 800 MHz
B - At the input frequency of 1000 MHz
C - At the input frequency of 1200 MHz

contour plot of intensity fluctuations ranging from -0.1 to -20.1 dB at 5 dB intervals where the input aperture is rectangular in shape and all radiating elements weighted equally.

By looking at the plots it is easy to measure the focus locations, depth of focus and the level and position of side lobes, and various other anomalies as a function of frequency (location). As is shown depth of focus increases at lower frequencies while at the same time the focus shifts inside.

Figure 6 is a similar dB plot when the input aperture is weighted by a one dimensional Hamming window of the form

$$H(U) = 0.54 + 0.46 \cos\left(\frac{2\pi\ (U - W)}{D}\right) \qquad (15)$$

is used.

As can be seen, application of Hamming window causes considerable suppression of the side lobes leading to a rather uniform taper at the output transducer plane.

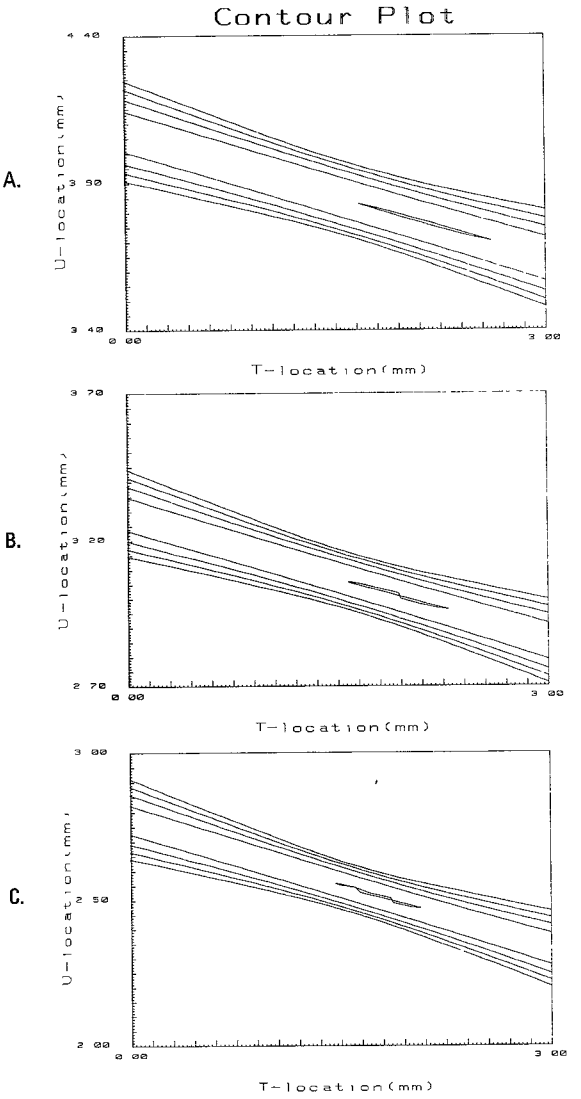

Figure 6. Decibel contour plot of field intensity in the vicinity of output transducer plane of figure 4. At the input frequency of A) 800 MHz, B) 1000 MHz. and C) 1200 MHz.

Comparing figures 5 and 6, one notices the relative shift in the focus and the steering angles. The shift in steering angles is illustrated in figure 7 where the spatial lateral locations versus peak modulation response for input frequencies from 700 to 1300 MHz is plated for both cases, indicating lower steering angles for the apodized case.

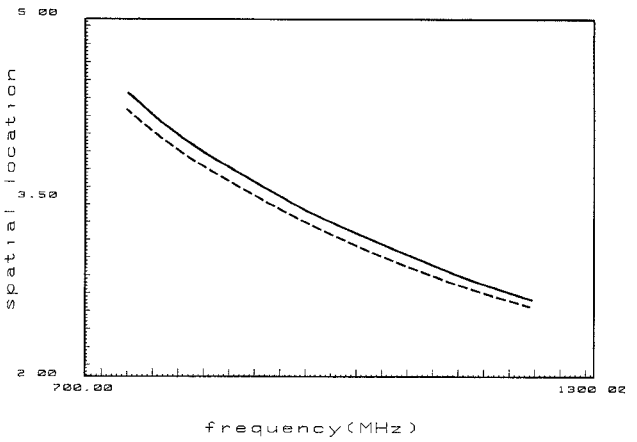

Figure 7. Latteral focus location versus input frequency for uniform aperture (solid curve) and apodized aperture (dashed curve).

In conclusion, the work presented in this paper deals with the diffraction process in BAW channelizers/spectrum analyzers. We have formulated a general approach to wave diffraction based on Huygen's principle. The approach provides the initial performance model, necessary to identify and characterize various design trade offs, helping the designer to overcome many of the challenges relevant to performance requirements. Validity and usefulness of the technique is demonstrated by computing the generalized wave disturbance due to both apodized and unapodized linear phased input array and a curved reflector. This approach, however, is valid for steering angles and propagation directions where parabolic approximation to slowness curves can be made.

Acknowledgement

This work was partially supported by the Naval Research Laboratory under NRL Contract N00019-85-C-2588.

REFERENCES

1. F. Sabet-Peyman, et al, "Beam Scanning and Focusing of Bulk Acoustic Waves," Proc. Ultrasonics Symposium, P. 424, 1984.

2. F. Sabet-Peyman and I.C. Chang," Diffraction and Detection of Bulk Acoustic Waves," Proc. SPIE Vol. 545, p. 58, 1985.

3. F. Sabet-Peyman and I.C. Chang," High Dynamic Range Bulk Acoustic Wave Channelizer," Proc. Ultrasonics Symposium, 1985.

4. I.C. Chang and S. Lee, "Efficient Wideband Acousto-Optic Bragg Cells," Proc. Ultrasonics Symposium, p. 427, 1983.

5. E.P. Papadakis, "Diffraction of Ultrasound Radiating into an Elastically Anisotropic Medium," J. Acous. Soc. Am., Vol. 36, p. 414, 1964.

6. M.G. Cohen, "Optical Study of Ultrasonic Diffraction and Focusing in Anisotropic Media," J. Appl. Phys., Vol. 38, p. 3821, 1967.

7. N.R. Ogg, "A Huygen's Principle for Anisotropic Media," J. Phys. A.: Gen. Phys., Vol. 4, p. 382, 1971.

8. M.S. Kharusi and G.W. Farnell, "On Diffraction and Focusing in Anisotropic Crystals," Proc. IEEE, Vol. 60, p. 945, 1972.

9. P.C. Waterman, "Orientation Dependence of Elastic Waves in Single Crystals," Phys. Rev. Vol. 113, p. 1240, 1959.

10. H. Seki, et al, "Diffraction Effects in the Ultrasonic Field of a Piston Source and Their Importance in the Accurate Measurement of Attenuation," J. Acous. Soc. Am., Vol. 28, p. 230, 1956.